Design of subwavelength superscattering nanospheres

Zhichao Ruan[a] and Shanhui Fan
Ginzton Laboratory, Department of Electrical Engineering, Stanford University, Stanford, California 94305, USA

(Received 15 August 2010; accepted 4 December 2010; published online 24 January 2011)

We design a subwavelength superscattering nanosphere with plasmonic-dielectric-plasmonic layer structure. We show that the scattering cross section of such a particle can be significantly enhanced by employing multiple resonances with different total angular momenta, and by ensuring that all these resonances have almost the same frequency and operate in the overcoupling region. © *2011 American Institute of Physics*. [doi:10.1063/1.3536475]

Enhancing the scattering cross section of subwavelength nanoparticles has practical significance for applications such as imaging, biomedicine, and photovoltaics.[1–10] Most subwavelength nanoparticles have a scattering cross section less than $3\lambda^2/2\pi$ since the underlying resonance has a total angular momentum $l=1$.[2,4,6] In Ref. 10, it has been pointed out that one can achieve a cross section of $(2l+1)\lambda^2/2\pi$ where $l>1$, by instead employing a resonance with a larger total angular momentum of l. In this paper, building upon a previous work on a two-dimensional cylindrical scatterer,[11] we numerically demonstrate subwavelength spherical particles with a scattering cross section beyond $(2l+1)\lambda^2/2\pi$, by employing multiple resonances with different total angular momenta, and by ensuring that all these resonances have almost the same frequency and operate in the overcoupling region. Such a theoretical design is relevant since spherical nanoparticles have been widely explored experimentally in nanoplasmonics.[1–8]

We start by formulating the general theoretical idea in Ref. 11 specifically for individual spherical scatterers. We consider a spherical particle in air. To describe the scattering process, we expand the field outside of the sphere in terms of different channels labeled by (l,m,σ). Here, l is the total angular momentum, m corresponds to the angular momentum component along the z direction and is subject to $-l \le m \le l$, and σ labels polarizations. At each angular momentum (l,m), there are two orthogonal polarizations: transverse magnetic (TM) and transverse electric (TE). For a TM (TE) polarization, the magnetic (electric) fields can be written as $\mathbf{H}_{TM}=\sqrt[4]{\frac{\varepsilon_0}{\mu_0}}\nabla\times\hat{\mathbf{r}}\Phi_{TM}$ $\left(\mathbf{E}_{TE}=\sqrt[4]{\frac{\mu_0}{\varepsilon_0}}\nabla\times\hat{\mathbf{r}}\Phi_{TE}\right)$, where $\Phi_{TM}(\Phi_{TE})$ is proportional to the electric (magnetic) potential and satisfies the scalar wave equation in the spherical coordinate.[12] Using such an expansion, in general, the potentials in the air region outside the scatterer can be written as

$$\Phi_\sigma=\sum_{l=1}^{\infty}\sum_{m=-l}^{l}A_{l,m}(a^+_{l,m,\sigma}h_l^{(2)}(kr)+a^-_{l,m,\sigma}h_l^{(1)}(kr))\times P_l^{|m|}(\cos\theta)\exp(im\phi), \quad (1)$$

where $A_{l,m}$ is a normalization constant, (r,θ,ϕ) are the spherical coordinates oriented at the center of the particle, k is the wave number in air, $h_l^{(1)}$ $(h_l^{(2)})$ is the l-th order spherical Hankel function of the first (second) kind, and P_l^m is the associated Legendre function of the first kind. Here the summation excludes the $l=0$ term because such a term is a function of r only, and hence does not contribute to the electromagnetic field. Since $h_l^{(1,2)}(kr)\to e^{i(l\pi/2+\pi/4)}e^{(+,-)ikr}/kr$, taking the convention that the field varies in time as $\exp(-i\omega t)$, one can identify $a^+_{l,m,\sigma}$ and $a^-_{l,m,\sigma}$ as the incoming and outgoing wave amplitudes. By integrating the Poynting vector over a closed spherical surface at $r=\infty$, we obtain the power carried in the incoming or outgoing waves in each channel,

$$P^{\pm}_{l,m,\sigma}=\frac{2\pi}{k^2}\frac{l(l+1)}{(2l+1)}\frac{(l+|m|)!}{(l-|m|)!}|A_{l,m}|^2|a^{\pm}_{l,m,\sigma}|^2. \quad (2)$$

Therefore, by choosing the normalization constant

$$A_{l,m}=k\sqrt{\frac{1}{2\pi}\frac{(2l+1)}{l(l+1)}\frac{(l-|m|)!}{(l+|m|)!}}, \quad (3)$$

we have then $|a^+_{l,m,\sigma}|^2$ and $|a^-_{l,m,\sigma}|^2$ representing the incoming and outgoing power carried by the waves in the (l,m,σ) scattering channel.

For a scatterer with a spherical symmetry, amplitudes in different channels do not mix with one another. Thus, for each channel, we define the reflection coefficient $R_{l,\sigma}$ as

$$R_{l,\sigma}\equiv\frac{a^-_{l,m,\sigma}}{a^+_{l,m,\sigma}}. \quad (4)$$

Note that due to the spherical symmetry, $R_{l,\sigma}$ is a function of σ and l, but not m. Moreover, by energy conservation,

$$|R_{l,\sigma}|\le 1. \quad (5)$$

We now calculate the scattering and absorption cross sections of the obstacle. For this purpose, by considering a x-polarized plane wave propagating along the z direction, i.e., $\mathbf{E}_{inc}=\hat{\mathbf{e}}_x\exp(ikz)$. The incident field can be described in terms of both electric and magnetic potentials,[12]

$$\Phi^{inc}_\sigma=\sum_{l=1}^{\infty}\sum_{m=-1,1}B_\sigma\sqrt[4]{\frac{\varepsilon_0}{\mu_0}}\frac{i^l}{2}\frac{(2l+1)}{l(l+1)}j_l(kr)P_l^{|m|}(\cos\theta)e^{im\phi}, \quad (6)$$

where $B_\sigma=1$ and i for the TM and TE polarizations, respectively. Similarly, the potentials for the scattered field outsider the scatterer are

$$\Phi^{sct}_\sigma=\sum_{l=1}^{\infty}\sum_{m=-1,1}B_\sigma\sqrt[4]{\frac{\varepsilon_0}{\mu_0}}\frac{i^l}{2}\frac{(2l+1)}{l(l+1)}S_{l,\sigma}h_l^{(1)}(kr)\times P_l^{|m|}(\cos\theta)e^{im\phi}, \quad (7)$$

where $S_{l,\sigma}$ is the scattering coefficient for the (l,m,σ) scat-

[a]Electronic mail: zhichao@stanford.edu.

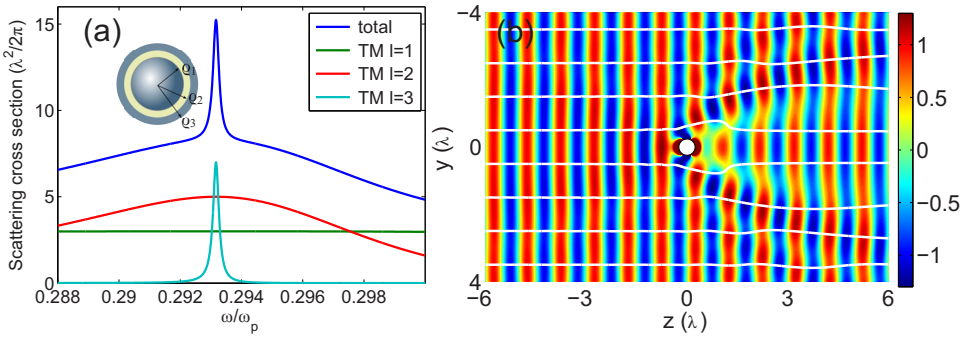

FIG. 1. (Color online) (a) Total scattering cross section of a nanosphere in the lossless case, and the contributions from individual channels. (Inset) Schematic of the nanosphere. The dark (dark cyan) and gray (yellow) areas correspond to a plasmonic material and a dielectric, respectively. The permittivity of dielectric is $\varepsilon_d=12.96$. The geometric parameters are $\rho_1=0.4749\lambda_p$, $\rho_2=0.6404\lambda_p$, and $\rho_3=0.8249\lambda_p$, where $\lambda_p=2\pi c/\omega_p$, with c being the speed of light in vacuum. (b) Real part of the total E_x field distribution and the "flow lines" of Poynting vector at a frequency of $0.2932\omega_p$, where a plane wave with unity amplitude illuminates the nanosphere from the left side. The white circle at the center indicates the sphere.

tering channel. Noting that $\Phi_\sigma=\Phi_\sigma^{inc}+\Phi_\sigma^{sct}$, and comparing Φ_σ to Eq. (1), we have

$$S_{l,\sigma}=\frac{R_{l,\sigma}-1}{2}. \tag{8}$$

Furthermore, the scattered power in the $(l,m=\pm 1,\sigma)$ scattering channel is

$$P_{l,m,\sigma}^{sct}=\left|B_l\sqrt[4]{\frac{\varepsilon_0}{\mu_0}}\frac{i^l}{2}\frac{(2l+1)}{l(l+1)}S_{l,\sigma}\right|^2/|A_{l,m}|^2$$
$$=\frac{\pi}{2k^2}\sqrt{\frac{\varepsilon_0}{\mu_0}}(2l+1)|S_{l,\sigma}|^2. \tag{9}$$

As a result, the total scattering cross section is

$$C^{sct}\equiv\frac{P^{sct}}{I_0}=\sum_\sigma\sum_{l=1}^{\infty}\frac{\lambda^2}{2\pi}(2l+1)|S_{l,\sigma}|^2=\sum_\sigma\sum_{l=1}^{\infty}\frac{\lambda^2}{2\pi}(2l+1)$$
$$\times\left|\frac{R_{l,\sigma}-1}{2}\right|^2, \tag{10}$$

and the total absorption cross section is

$$C^{abs}\equiv\frac{P^{abs}}{I_0}=\sum_\sigma\sum_{l=1}^{\infty}\frac{\lambda^2}{8\pi}(2l+1)[1-|R_{l,\sigma}|^2]. \tag{11}$$

Using Eq. (5), one can immediately infer that for given polarization, the total contributions of all channels with total angular momentum l cannot exceed $(2l+1)\lambda^2/2\pi$ for the scattering cross section, and $(2l+1)\lambda^2/8\pi$ for the absorption cross section. The strongest scattering occurs when $R_{l,\sigma}=-1$, while the strongest absorption occurs when $R_{l,\sigma}=0$.

For subwavelength particles, typically only those channels that support resonances have significant contributions to the total cross sections. When a resonance is present in a scattering channel labeled by (l,m,σ), the scattering process can be modeled by temporal coupled-mode equations, which leads to a general formula for the reflection coefficient[13,14]

$$R_{l,\sigma}=\frac{i(\omega_0-\omega)+\gamma_0-\gamma}{i(\omega_0-\omega)+\gamma_0+\gamma}. \tag{12}$$

Here ω is the frequency of the incident wave, ω_0 is the resonant frequency, γ_0 is the intrinsic loss rate due to material absorption, and γ is the external leakage rate due to the coupling of the resonance to the outgoing wave. All these parameters for the resonance are dependent of l and σ. As a result, using Eq. (9) and summing over the $m=\pm 1$ channels, the total contribution of all channels with the same total angular momentum l becomes

$$C_{l,\sigma}^{sct}=(2l+1)\frac{\lambda^2}{2\pi}\frac{\gamma^2}{(\omega-\omega_0)^2+(\gamma_0+\gamma)^2}. \tag{13}$$

In the absence of resonance in other angular momentum channels, the total scattering cross section thus exhibits a Lorentzian spectral line shape, reaching a peak value of $(2l+1)\frac{\lambda^2}{2\pi}\frac{\gamma^2}{(\gamma_0+\gamma)^2}$ at the resonant frequency ω_0. In the strong overcoupling regime, i.e., $\gamma\gg\gamma_0$, the total scattering cross section maximizes to $(2l+1)\lambda^2/2\pi$.

From the analysis above, one strategy of designing nanoparticles with a large scattering cross section is to create resonance in channels with high total angular momentum.[10] Instead of doing so, following the theoretical suggestion of Ref. 11, we seek to create accidental degeneracy of resonant modes with different total angular momenta. Compared with the approach in Ref. 10, one potential advantage of the present approach is that one can exploit channels with smaller total angular momentum, which are typically less susceptible to loss and more stably stay in the overcoupling region.[11] Here we refer to a subwavelength particle having a total scattering cross section exceeding $(2l_{max}+1)\lambda^2/2\pi$ as a superscatterer, where l_{max} is the maximal total angular momentum involved.

To design a superscatterer, we consider a nanosphere which consists of concentric metal-dielectric-metal layer [Inset of Fig. 1(a)]. The metal is described by a Drude model $\varepsilon_m=1-\omega_p^2/(\omega^2+i\gamma_d\omega)$. We start with lossless case first by setting $\gamma_d=0$. We note that a similar layer structure has been applied to design a superscattering nanorod in two dimensions.[11] Here we show that the same idea can be adopted for three-dimensional design as well. With a proper choice of the dielectric layer thickness, for the modes with the magnetic field parallel with the interface, the corresponding planar structure (the left-top inset of Fig. 2) exhibits a flat band around the frequency of $0.2932\omega_p$ (solid lines in Fig. 2). In the nanosphere, when the waves propagate along the equator, i.e., $m=\pm l$, the resonances are of the whispering gallery type. (As an example, the TM resonance with $l=3$, $m=3$ is shown in the right-bottom inset of Fig. 2.) Moreover, since the modes with the same l but different m

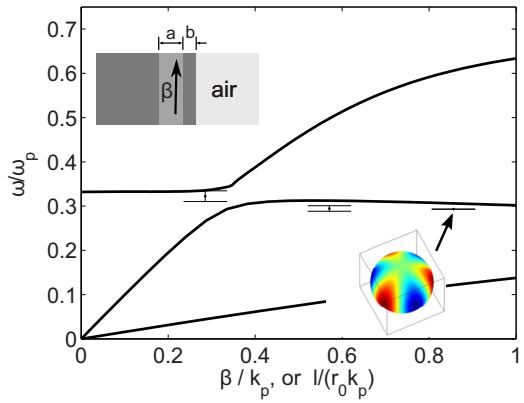

FIG. 2. (Color online) The band structure of the corresponding plane structure shown in the left-top inset (lines), and the resonant frequencies and the leakage rates for the $l=1,2,3$ TM modes in the sphere (bars). The center and the height of each bar correspond to the resonant frequency and the leakage rate, respectively. In the inset, $a=\rho_2-\rho_1$, $b=\rho_3-\rho_2$. The right-bottom inset shows the H_θ field distribution for the ($l=3$, $m=3$, TM) resonant mode.

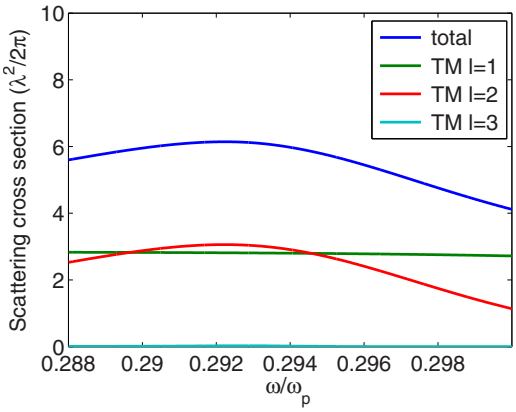

FIG. 3. (Color online) Total scattering cross section in the lossy case, and the contribution from each individual channel.

are all degenerate, the resonant frequency of a mode with total angular momentum l can therefore be determined by using

$$\beta \cdot 2\pi r_0 = 2\pi l, \tag{14}$$

where $r_0=(\rho_1+\rho_2)/2$, and β is the propagation constant in the corresponding planar structure. As a result, the existence of a flat band in the corresponding planar structure should directly translate into near-degeneracy in the nanosphere between modes with different total angular momenta.

We plot the resonant frequencies and the leakage rates of the TM modes of the nanosphere, as a function of l/r_0 in Fig. 2. We indeed observe resonances in the $l=1,2,3$ channels, all lying close to the frequency of $0.2932\omega_p$ where the planar structure has a flat band. The positions of these resonances in general agree quite well with Eq. (14). Also, the leakage rates of these resonances decrease as the total angular momentum increases, in consistency with Refs. 10 and 15.

We now calculate the total scattering cross section of the nanosphere [Fig. 1(a)]. The total scattering cross section reaches a peak value of $15.2(\lambda^2/2\pi)$ or $2.42\lambda^2$ at the frequency of $0.2932\omega_p$, in comparison to the geometric cross section of the particle of $0.18\lambda^2$, for such a subwavelength particle with a diameter of 0.485λ. In consistency with Eq. (13), the contribution from different total angular momentum l each has a Lorenztian lineshape that peaks with a value of $(2l+1)\lambda^2/2\pi$, at a frequency around $0.2932\omega_p$ [Fig. 1(a)]. The total cross section also exceeds $7\lambda^2/2\pi$ where $l_{max}=3$. We have thus indeed designed a superscattering nanosphere.

Figure 1(b) shows the real part of E_x field distribution, when a plane wave with a frequency of $0.2932\omega_p$ and unity amplitude illuminates the nanosphere from the left side. The nanosphere leaves a significant shadow behind it, where the field strength is reduced. The "flow lines" of the Poynting vector field indicate significant redistribution of the power flow around the nanosphere.

We now consider the lossy case, by setting $\gamma_d=\gamma_{bulk}+A\times V_F/l_r$ in order to take into account both the bulk and the surface scattering effects for the electrons.[16] Here $\gamma_{bulk}=0.002\omega_p$ is appropriate for bulk silver at the room temperature,[17] $A\approx 1$,[16] $V_F=7.37\times 10^{-4}\lambda_p\omega_p$ is the Fermi velocity for silver,[18] and l_r is the electron mean free path. For this structure, $l_r=\rho_1$ is taken for the metallic core, and $l_r=\rho_3-\rho_2$ for the metallic shell. The total scattering cross section at the peak frequency of $0.2932\omega_p$ is reduced to $6.1\lambda^2/2\pi$ (Fig. 3), which nevertheless still exceeds $(2l_{max}+1)\lambda^2/2\pi$, since the contributions to scattering are mostly from the $l=1,2$ channels. The resonances with $l=3$ do not contribute, since they are no longer in the overcoupling regime due to the material loss. To summarize, our results show that a superscattering nanosphere can be designed even in the presence of realistic loss.

The authors acknowledge the support of the Interconnect Focus Center, funded under the Focus Center Research Program (FCRP), a Semiconductor Research Corporation entity, and the DOE Grant No. DE-FG 07ER46426.

[1] S. Nie and S. R. Emory, Science **275**, 1102 (1997).
[2] J. B. Jackson and N. J. Halas, Proc. Natl. Acad. Sci. U.S.A. **101**, 17930 (2004).
[3] L. R. Hirsch, R. J. Stafford, J. A. Bankson, S. R. Sershen, B. Rivera, R. E. Price, J. D. Hazle, N. J. Halas, and J. L. West, Proc. Natl. Acad. Sci. U.S.A. **100**, 13549 (2003).
[4] J. Aizpurua, P. Hanarp, D. S. Sutherland, M. Käll, G. W. Bryant, and F. J. Garcia de Abajo, Phys. Rev. Lett. **90**, 057401 (2003).
[5] F. Hao, Y. Sonnefraud, P. Van Dorpe, S. A. Maier, N. J. Halas, and P. Nordlander, Nano Lett. **8**, 3983 (2008).
[6] R. Bardhan, S. Mukherjee, N. A. Mirin, S. D. Levit, P. Nordlander, and N. J. Halas, J. Phys. Chem. C **114**, 7378 (2010).
[7] H. R. Stuart and D. G. Hall, Appl. Phys. Lett. **73**, 3815 (1998).
[8] S. Pillai, K. R. Catchpole, T. Trupke, and M. A. Green, J. Appl. Phys. **101**, 093105 (2007).
[9] H. A. Atwater and A. Polman, Nature Mater. **9**, 205 (2010).
[10] M. Tribelsky and B. Lukyanchuk, Phys. Rev. Lett. **97**, 263902 (2006).
[11] Z. Ruan and S. Fan, Phys. Rev. Lett. **105**, 013901 (2010).
[12] W. C. Chew, *Waves and Fields in Inhomogeneous Media* (IEEE Press, Piscataway, NJ, 1995).
[13] R. E. Hamam, A. Karalis, J. D. Joannopoulos, and M. Soljačić, Phys. Rev. A **75**, 053801 (2007).
[14] Z. Ruan and S. Fan, J. Phys. Chem. C **114**, 7324 (2010).
[15] H. C. van de Hulst, *Light Scattering by Small Particles* (Dover, New York, 1981).
[16] R. D. Averitt, D. Sarkar, and N. J. Halas, Phys. Rev. Lett. **78**, 4217 (1997).
[17] M. Ordal, L. Long, R. Bell, S. Bell, R. Bell, and R. Alexander, Appl. Opt. **22**, 1099 (1983).
[18] C. Kittel and P. McEuen, *Introduction to Solid State Physics* (Wiley, New York, 1996).